Graphical Abstract

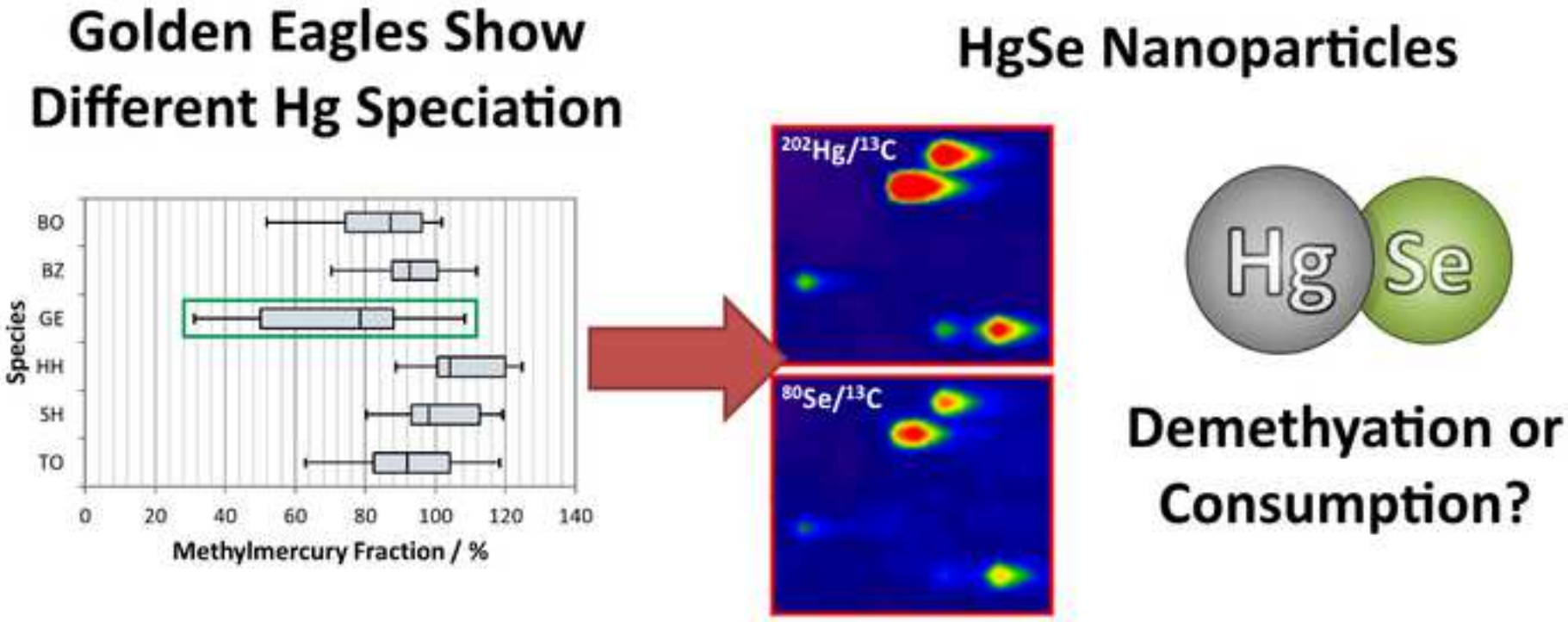

Mercury speciation in Scottish raptors reveals high proportions of inorganic mercury in Scottish golden eagles *(Aquila chrysaetos):* potential occurrence of mercury selenide nanoparticles

Highlights:

- Mercury speciation was studied in the livers of six species of terrestrial birds of prey.
- Golden eagles showed significantly lower methylmercury fractions.
- Stable isotopes indicate that the elevated inorganic mercury is marine-influenced.
- Bioimaging revealed potential evidence of mercury selenide nanoparticles.

Mercury speciation in Scottish raptors reveals high proportions of inorganic mercury in Scottish golden eagles *(Aquila chrysaetos):* potential occurrence of mercury selenide nanoparticles

Shaun T. Lancaster[a,b,1]*, Gabriela Peniche[c], Ali Alzahrani[a], Magdalena Blanz[a,d], Jason Newton[e], Mark A. Taggart[f], Warren T. Corns[b], Eva M. Krupp[a], and Jörg Feldmann[a,g]

[a]Trace Element Speciation Laboratory Aberdeen (TESLA), Department of Chemistry, Meston Walk, University of Aberdeen, Aberdeen AB24 3UE, UK.

[b]PS Analytical, Crayfields Industrial Estate, Main Road, Orpington, Kent BR5 3HP, UK

[c]The Royal (Dick) School of Veterinary Studies, The University of Edinburgh, Easter Bush Campus, Midlothian, Edinburgh, EH25 9RG, UK

[d]Archaeology Institute, University of the Highlands and Islands, Orkney College UHI, Kirkwall, Orkney, KW15 1LX, Scotland, UK

[e]National Environmental Isotope Facility, Scottish Universities Environmental Research Centre (SUERC), East Kilbride, G75 0QF, UK

[f]The Environmental Research Institute (ERI), University of Highlands and Islands, Castle St, Thurso, KW14 7JD, UK

[g]TESLA – Analytical Chemistry, Institute of Chemistry, Universitaetsplatz 1, University of Graz, 8010 Graz, Austria

[1]Present address: Department of General, Analytical and Physical Chemistry, Chair of General and Analytical Chemistry, Montanuniversität Leoben, 8700 Leoben, Austria.

Abstract

Knowledge of the uptake and fate of mercury (Hg) compounds in biota is important in understanding the global cycling of Hg and its transfer pathways through food chains. In this study, we analysed total mercury (T-Hg) and methylmercury (MeHg) concentrations in 117 livers of Scottish birds of prey that were found across Scotland and submitted for post-mortem examination through the Raptor Health Scotland project between 2009–2019. Statistical comparisons focussed on six species (barn owl, *Tyto alba*; Eurasian common buzzard, *Buteo buteo*; golden eagle, *Aquila chrysaetos*; hen harrier, *Circus cyaneus*; Eurasian sparrowhawk, *Accipiter nisus*; and tawny owl, *Strix aluco*) and showed that golden eagles had a statistically lower fraction of MeHg compared to other raptor species. Further investigation using stable carbon and stable nitrogen isotope ratio measurements carried out for the golden eagles (n = 15) indicated that the increased presence of inorganic mercury (iHg) correlated with a marine influence on the primarily terrestrial diet. Additional bioimaging (n = 1) with laser ablation – inductively coupled plasma – mass spectrometry indicated the co-location of Hg and selenium (Se) within the liver tissue and transmission electron microscopy showed evidence of nanoparticles within the range of 10–20 nm. Further analysis using single particle – inductively coupled plasma – mass spectrometry (n = 4) confirmed the presence of Hg nanoparticles. Together, the evidence suggests the presence of mercury selenide (HgSe) nanoparticles in the liver of some golden eagles that, to our knowledge, has never been directly observed in terrestrial birds of prey. This study points to two alternative hypotheses: these golden eagles may be efficient at breaking down MeHg and form HgSe nanoparticles as a detoxification mechanism (as previously observed in cetaceans), or some golden eagles with elevated iHg may have accumulated these nanoparticles by foraging on stranded cetaceans or seabirds.

Keywords: Mercury, Methylmercury, Nanoparticles, Raptors, Birds of prey

1. Introduction

Mercury (Hg) is a well-studied, ubiquitous pollutant of global concern (Obrist et al., 2018). Although naturally occurring, it is anthropogenic emissions that make up the majority of Hg pollution present in the modern environment (UN Environment, 2019). Recently, the Minamata Convention came into force (in 2017) with the aim to reduce emissions of Hg into the environment (UN Environment, 2017). Once released, readily volatile Hg cycles around the globe, and can deposit in different environmental sinks (either by wet or dry deposition) and cause detrimental effects to wildlife (Day et al., 2005; Evers et al., 2008; Lurz et al., 2017). The most common exposure pathway is through diet, whereby up to 16% of inorganic mercury (iHg) (Syversen and Kaur, 2012) and 100% of methylmercury (MeHg) (Gochfeld, 2003) ingested is liberated from the matrix and absorbed by the gastro-intestinal tract. Therefore, MeHg tends to pose the most significant threat to humans (Mergler et al., 2007) and wildlife (Chételat et al., 2020; Scheuhammer et al., 2007) due to its high absorption rate, toxicity and propensity to bioaccumulate.

Birds of prey, also known as raptors, can be exposed to Hg in both terrestrial (Cristol et al., 2008) and aquatic (Eagles-Smith et al., 2009a) environments. Exposure to Hg can cause immunological, physiological, and behavioural changes (Carlson et al., 2014; Scheuhammer et al., 2007; Seewagen et al., 2019). Previous literature on Hg in birds of prey has focussed on the fate of MeHg after uptake through the diet. Once consumed, MeHg cycles within the blood stream and accumulates primarily in the liver and kidneys (Kenow et al., 2007). Toxic effects can be naturally mitigated by elimination and excretion of MeHg, which can occur via different routes. Primary elimination routes include sequestering to feathers (which are then shed during moulting), urinary and faecal excretion (Bearhop et al., 2000; Lewis and Furness, 1993, 1991). In female birds, maternal transfer of MeHg to eggs can also occur (Ackerman et al., 2020). The half-life of MeHg in the bloodstream has been shown to change over time, with initially rapid decreases observed (during the first 24 hours following exposure), followed by much slower subsequent decay times (>45 days) (Monteiro and Furness, 2001). Hepatic demethylation of MeHg has also been proposed (Eagles-Smith et al., 2009b; Henny et al., 2002; Scheuhammer et al., 1998). Accumulation of iHg in the liver is often interpreted as evidence of such

hepatic demethylation, which may subsequently bind with selenium (Se) in the liver. Such interactions can exist in different forms, such as the Hg-selenocysteine complex (1:4 stoichiometry) found recently in seabirds (Manceau et al., 2021b), which is formed from the demethylation of MeHg (Manceau et al., 2021a) and acts as an intermediate step to the formation of mercury selenide (HgSe) nanoparticles that may accumulate in the liver. However, direct observations of such HgSe nanoparticles have, so far, only been reported in cetaceans (Bolea-Fernandez et al., 2019; Gajdosechova et al., 2016) and, very recently, seabirds (Manceau et al., 2021b; Renedo et al., 2021), who typically have a very high dietary intake of MeHg.

Most literature regarding Hg speciation in wildlife generally neglects dietary uptake of iHg given that MeHg is more readily absorbed through the diet and more toxic. Bioaccumulation of Hg via iHg is possible at the lower trophic levels of the food chain (Bouland et al., 2012), as well as the top levels (Palma et al., 2005), For this reason, iHg speciation and monitoring of concentrations of total mercury (T-Hg) at higher trophic levels of the food chain, in this case Scottish raptors, may provide additional clues to potential uptake mechanisms or pathways. The consumption of iHg and MeHg may vary across the different birds of prey depending on the species' diet habits (small birds feeding on insects, rodents, carrion, marine based, etc.). In largely terrestrial birds of prey, high iHg concentrations may (for example) be indicative of dietary uptake, novel Hg exposure pathways, or hepatic demethylation.

In avian ecology (and less so ecotoxicology), stable isotope ratios are frequently used to help identify different food sources; most notably, stable carbon ($\delta^{13}C$) and nitrogen ($\delta^{15}N$) isotope ratios. The isotopic ratios of the consumer tissues depend on the isotope ratios of their diet, which, for a terrestrial diet, is subsequently dependant on available plant species. $\delta^{13}C$ ratios show very limited enrichment following consumption and tend to differ markedly between terrestrial C_3 plant ecosystems and marine ecosystems, whereas $\delta^{15}N$ generally shows enrichment of 2–4 ‰ with each increase in trophic level (Inger and Bearhop, 2008; Zanden et al., 1999). Animals in marine ecosystems tend to have elevated $\delta^{15}N$ values when compared to terrestrial animals due to a combination of

longer food chains in the marine environment and higher $\delta^{15}N$ in marine plants at the base of the food chains (Schoeninger and DeNiro, 1984). For these reasons, $\delta^{13}C$ is widely used to identify relative contributions made to diet by marine- vs terrestrial-derived foods (Chisholm et al., 1982; Hobson and Clark, 1992; Kelly, 2000) and $\delta^{15}N$ is used to infer trophic level in avian ecology studies (Cherel et al., 2005; Hobson and Clark, 1992; Kelly, 2000). More infrequently, stable sulphur isotope ratios ($\delta^{34}S$) have also been used similarly to infer relative contributions of marine and terrestrial environments (Hebert et al., 2008).

Bioimaging with laser ablation – inductively coupled plasma – mass spectrometry (LA-ICP-MS) has been used extensively to assess the location and correlation of elements in biological tissues (Becker et al., 2014), such as to show the correlation of Hg and Se (as HgSe nanoparticles) within the livers of pilot whales (Gajdosechova et al., 2016). However, the resolution of the technique typically ranges from 10–100 µm, which is not sufficient to determine accurate sizes of nanoparticles. Complimentary techniques may be used in parallel to give further insight to inorganic particulates on the nano-scale, such as single particle (sp)-ICP-MS. Here, dilute solutions containing analyte nanoparticles are analysed with extremely short dwell times, such that statistically each spike in signal corresponds to one packet of ions from a single particle (Meermann and Nischwitz, 2018). Although the technique provides excellent detection capabilities, it suffers greatly from the lack of ability for simultaneous determinations of two elements when using quadrupole-based mass spectrometers. Another complimentary technique is transmission electron microscopy (TEM), which has been used to study the size and morphology of nanoparticles (Rauwel et al., 2015). Together, these techniques can be used to gain further insights into the fate of Hg in biological samples.

Here, we investigate Hg presence and speciation in the livers of birds of prey to further understand potential exposure routes and fate of Hg in the environment. To achieve this, we analysed T-Hg and its speciation in 117 liver samples from raptors of 13 different species from across Scotland. Statistical comparisons were carried out between six raptor species (with more than seven individuals): for barn

owl, *Tyto alba*; Eurasian common buzzard, *Buteo buteo*; golden eagle, *Aquila chrysaetos*; hen harrier, *Circus cyaneus*; Eurasian sparrowhawk, *Accipiter nisus*; and tawny owl, *Strix aluco*. Further investigation was carried out for golden eagles using carbon, nitrogen, and sulphur stable isotope ratios (n = 15) to consider diet, and nanoparticle analysis by sp-ICP-MS (n = 4), as well as bioimaging using LA-ICP-MS and TEM (n = 1) to consider the form of Hg and its location and interaction with Se. Following interpretation of results, we present evidence that iHg speciation (alongside MeHg) may give additional indications regarding different Hg uptake mechanisms and food chain transfer pathways in Scottish golden eagles.

2. Methods and materials

2.1. Bird collection and sampling

Raptor liver tissues (n = 117) used for chemical analyses originated from raptor carcasses found across Scotland (Figure A.1, Table A.1) between 2009–2019, which were submitted for post-mortem examination through the Raptor Health Scotland project led by the Royal (Dick) School of Veterinary Studies (University of Edinburgh, UK). Tissues were collected and stored in polypropylene containers at −20 °C prior to further processing.

2.2. Sample preparation and storage

For all chemical determinations, approximately 1 g of fresh liver samples were freeze dried and then ground into a fine powder using a mortar and pestle. Moisture content was determined by weight loss using weights taken before and after freeze drying. All reagents used were of analytical grade.

Bioimaging measurements carried out on 30 µm thin sections of liver cut using a Bright 5030 microtome cryostat (Bright Instruments, UK). All samples were subsequently stored in a freezer at −8 °C prior to analysis.

2.3. Sample analysis

2.3.1. MeHg quantification

MeHg extraction and analysis by liquid chromatography – photochemical vapour generation – atomic fluorescence spectrometry (LC-PVG-AFS) (Lancaster et al., 2019) was carried using a PSA 10.820 speciation system and PSA Millennium Merlin analyser (PS Analytical, UK). 30–50 mg of liver sample was extracted with 5 mL of a solution containing 10 mM ammonium pyrrolidine dithiocarbamate in 80% methanol in a hot block digestor (DigiPREP; SCP Science, Canada) at 60 °C for 30 min, followed by 15 min ultrasonication (Ultrasonic Cleaner, Model 010; Skymen, China). Samples were filtered using 0.45 µm PTFE filters (Chromacol Filter PTFE 30-SF-45(T); Thermo Scientifc, USA), diluted, and analysed using the LC-PVG-AFS method described with 25% acetic acid and UV to reduce the Hg species to elemental mercury (Hg^0). Blank extractions were prepared in duplicate alongside the samples and monitored for MeHg, however limit of detection (LOD) was calculated using the standard error of the calibration intercept.

2.3.2. Total Hg and Se quantification

T-Hg determination was carried out using a PSA Millennium Merlin (PS Analytical, UK) analyser. 30–50 mg of liver sample was pre-digested overnight in 3 mL of concentrated nitric acid. Before the samples were subjected to open-vessel digestion, 2 mL concentrated hydrogen peroxide was added. The samples were digested using a hot block digestor (DigiPREP; SCP Science, Canada) at 50 °C for 5 min before the temperature was ramped to 100 °C over 25 min. The samples were left to digest for a further 30 minutes at 100 °C. After digestion, the samples were allowed to cool at room temperature and the lids removed to allow the nitrous fumes to discipate. The samples were then diluted to 20 mL and filtered using Whatman™ filter papers (41, Ashless, 90 mm diameter; Fisher Scientific, UK). After filtration, the samples were diluted to 40 mL with deionised water. Any MeHg remaining in the sample was converted to iHg with the addition of 1 mL concentrated hydrochloric acid and 2 mL of 0.1N bromide/bromate solution. After 30 min, the samples were decolourised with 35 µL of 12% (m/v) hydroxylamine hydrochloride and diluted to 50 mL. A 10 mL aliquot of the sample was taken for further processing for total selenium (T-Se) determination. T-Hg analysis was carried out using cold

vapour (CV)-AFS, where a solution of 2% (m/v) tin(II) chloride in 1.2 M hydrochloric acid was used to convert the Hg to Hg^0.

T-Se analysis was carried out using a PSA Millennium Excalibur analyser (PS Analytical, UK). Following preparation for T-Hg, the 10 mL aliquot of the sample was further digested in 10 mL HCl by open-vessel digestion in the hot block digester at 120 °C for 1 hour. The samples were allowed to cool at room temperature before diluting to 50 mL, where they were then analysed by hydride generation (HG)-AFS. The Se-hydrides were generated by the addition of 0.2 M sodium borohydride in 0.1 M sodium hydroxide. Digestion blanks for T-Hg and T-Se were prepared in duplicate and the LOD was determined using replicate measurements of the digestion blanks.

2.3.3. Isotope ratio analysis

Stable isotope ratios of carbon, nitrogen, and sulphur in freeze dried golden eagle liver samples (n = 15) were analysed. Subsamples of 2.5–2.9 mg were weighed into 3 × 5 mm tin capsules and sequentially analysed for $\delta^{15}N$, $\delta^{13}C$, and $\delta^{34}S$ using a PyroCube elemental analyser (Elementar, Hanau, Germany) interfaced with an Elementar VisION isotope ratio mass spectrometer (Skinner et al., 2019). Stable isotope ratios reported here use the delta (δ) notation (McKinney et al., 1950), which for $\delta^{13}C$, $\delta^{15}N$, or $\delta^{34}S$ is: $[(R_{sample}/R_{standard}) - 1]$, where R is the ratio of the heavy to light isotope (e.g., $^{13}C/^{12}C$), and measured values are expressed in per mil (‰).

2.3.4. Nanoparticle characterisation by sp-ICP-MS

Approximately 20 mg of sample was first defatted using acetone. HgSe nanoparticles were extracted by enzymatic digestion (Gajdosechova et al., 2016) at 37 °C overnight using a solution of 1 mg mL^{-1} protease and 5 mg mL^{-1} SDS in 50 mM ammonium carbonate buffer (pH 7.4). The nanoparticles were isolated from the sample by filtration using centrifuge filters (Amicon Ultra, Merck, UK) with a 50 kDa cut-off spun at 11 300 × g. The filter was further washed with MilliQ water to remove dissolved Hg. The filtration residue was then removed and diluted in MilliQ water before analysis with sp-ICP-MS

using an Agilent 7900 series ICP-MS (Agilent Technologies, USA). Isotopes of ^{77}Se and ^{202}Hg were monitored individually for 2 min each with a 1 ms dwell time. Helium was added as a collision gas at 2 mL min^{-1}. Transport efficiency was determined by analysis of a gold nanoparticle reference material (NIST RM 8013, 60 nm nominal diameter), which was diluted to 50 ng L^{-1}. Particle number, particle sizes, and limit of size detection were calculated using the Agilent MassHunter software.

2.3.5. Elemental mapping of Hg and Se by LA-ICP-MS

Element mapping of Hg and Se present in tissues was undertaken using the thin sections of one golden eagle liver sample with LA-ICP-MS (Gajdosechova et al., 2016). Analysis was carried out using a New Wave UP-213 laser ablation system (New Wave Research, USA) coupled to an Agilent 7900 series ICP-MS (Agilent Technologies, USA). Laser energy of 30% and spot size of 55 µm was used. Ablation lines covering the entire liver section were generated of length 13.5 mm and spaced 60 µm apart with a scan speed of 50 µm s^{-1}. Mass to charge ratios of ^{13}C, ^{80}Se, and ^{202}Hg were monitored, with a dwell time of 0.010 s for ^{13}C and 0.490 s for ^{80}Se and ^{202}Hg. Argon carrier gas was used at 1.2 L min^{-1} and hydrogen reaction gas was used at 3.5 mL min^{-1}.

2.3.6. Bioimaging of nanoparticles by TEM

Thin sections of liver sample from one golden eagle were placed onto copper grids (TAAB, UK) and subject to TEM imaging using a JEOL-1400 plus electron microscope. An accelerating voltage of 80 kW and an AMP UltraVUE camera were used.

2.4. Quality control

Certified reference material DOLT-4 was used for validation of the MeHg, T-Hg, and T-Se determinations.

For isotope ratio measurements, international reference materials were placed at the start of the N/C/S run to correct for accuracy. Materials used were USGS40 (glutamic acid) (Coplen et al., 2006; Qi et al., 2003) for $\delta^{13}C$ and $\delta^{15}N$ and silver sulfide standards IAEA-S1, S2, and S3 for $\delta^{34}S$. These were

preceded by a suite of differently-sized MSAG2 (a solution of methanesulfonamide and gelatin) internal standards to correct for linearity (Werner and Brand, 2001). Two internal reference materials were placed every 10 samples: these included MSAG2, M2 (a solution of methionine, gelatin, glycine), and ^{15}N-enriched alanine and SAAG2 (a solution of sulfanilamide, gelatin, and ^{13}C-enriched alanine). The internal standards were designed to have a wide range of isotope compositions.

2.5. Statistics

2.5.1. Significance testing

Statistical tests were carried out using Minitab19. Data sets were tested for normal distribution using the Kolmogorov-Smirnov test with Lilliefors correction. Where the data sets displayed distributions that were not significantly different to a normal distribution, one way ANOVA was used for comparisons of three or more data sets, with Tukey's HSD tests applied post-hoc following a significant result ($p < 0.05$). Where distributions differred significantly from a normal distribution, Kruskal-Wallis (non-parametric) ANOVAs were used with Bonferroni corrected pairwise Mann-Whitney tests applied post-hoc.

2.5.2. Measurement uncertainty

The measurement uncertainty for the MeHg, T-Hg, and T-Se methods were determined using a bottom-up approach (JCGM 100:2008, 2008). The uncertainty contributions were taken from available certificates, or from statistical analysis of repeated measurements. Precision was evaluated by triplicate extraction of 10% of the liver samples prepared and analysed on separate days, encompassing both measurement error and the sampling error. The recovery uncertainty was evaluated using DOLT-4 reference material extracted and measured in triplicate on each analysis day. The bias was tested for significance using a t-test and the uncertainty inflated for low degrees of freedom (Barwick and Ellison, 1999). All dilutions were carried out by weight. The uncertainty in the reading of the analytical balance was evaluated from the calibration certificate and the repeatability

of weighing (González and Herrador, 2007). The uncertainty in the measured concentration of the sample due to the linear calibration was evaluated using the EURACHEM/CITAC formula (Ellison and Williams, 2012) without considering replicate sample measurements to avoid double counting from the precision component (Kadis, 2017). The purity of the Hg and Se analytical standards were evaluated from certificates with an assumed rectangular distribution. The purity of the MeHg compound was evaluated from the stated purity assuming a ramp distribution (Van Look and Meyer, 2002). Once all sources of uncertainty were estimated, the components were combined according to the law of propagation of uncertainty. The result was expressed as expanded uncertainty (*U(C)*) by multiplying the combined uncertainty by a coverage factor, k = 2, corresponding to a 95% confidence level.

3. Results

3.1. Hg in raptor livers

In total, 117 raptor liver samples were analysed for MeHg and T-Hg. All sample concentrations reported in this study are reported as mg kg^{-1} dry weight (dw). Quality control and precision data have been detailed in Table A.2. The average moisture concentration of the liver samples tested was 70.8 ± 4.1%. T-Hg concentrations in raptor livers varied by 3 orders of magnitude; from 0.0348 mg kg^{-1} (a golden eagle nestling) to 24.4 mg kg^{-1} (a juvenile hen harrier; Table A.3). Six species with large enough data sets (n ≥ 9) were selected for more detailed comparisons: barn owl (n = 19), Eurasian common buzzard (n = 34), golden eagle (n = 15), hen harrier (n = 11), Eurasian sparrowhawk (n = 15), and tawny owl (n = 9); total n = 103. Comparison of the results obtained are shown in Figure 1.

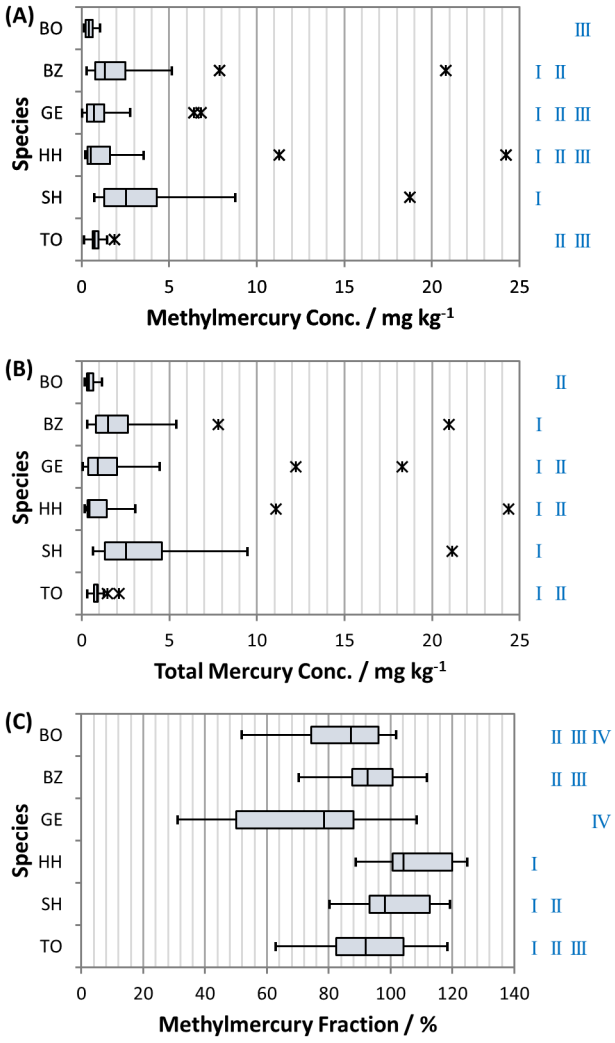

264

265 Figure 1 Box and whisker plots showing the range, semi-interquartile range, and median for
266 MeHg (A), T-Hg (B) and MeHg fraction (C) in barn owls (BO), buzzards (BZ), golden
267 eagles (GE), hen harriers (HH), sparrowhawks (SH), and tawny owls (TO). Outliers (in
268 A and B) exceeded 1.5 times the interquartile range. Roman numerals (in blue)
269 indicate the post-hoc groupings for each raptor species.

270 MeHg distributions for barn owl and tawny owl were normally distributed ($p > 0.15$), while all other
271 raptor species had non-normal distributions ($p < 0.05$). For T-Hg, all six species had non-normal
272 distributions. Therefore, for comparisons between species, non-parametric tests were used. ANOVAs
273 indicated differences between species for both MeHg and T-Hg results ($p < 0.0001$), however the post-
274 hoc tests revealed too many overlaps between species to highlight distinct differences. Assessment of

the measurement uncertainty for a typical analysis of MeHg and T-Hg in this study showed relative expanded uncertainties of 12.2% and 12.0% respectively (Table A.4a).

All species showed normally distributed MeHg fractions (proportion of T-Hg present as MeHg). ANOVAs indicated that there was a significant difference between species ($p < 0.0001$) in terms of MeHg fraction, and post-hoc tests indicated that golden eagles had significantly lower mean MeHg fractions than other species, except for barn owls. MeHg fractions up to 120% are covered within the combined measurement uncertainty of both analysis methods, however MeHg fractions determined to be >120% (hen harrier, n = 2) are outliers.

3.2. Stable isotope ratios ($\delta^{13}C$, $\delta^{15}N$ and $\delta^{34}S$) of golden eagle livers

Carbon, nitrogen, and sulphur stable isotope ratios plotted against iHg levels are shown in Figure 2 and Figure A.2–A.4. Sulphur stable isotope ratios showed no apparent relationship with iHg (Figure A.2). Comparisons were also made between the stable isotope data and MeHg, T-Hg, and the MeHg fraction data (Figure A.2–A.4), however, no trends were observed.

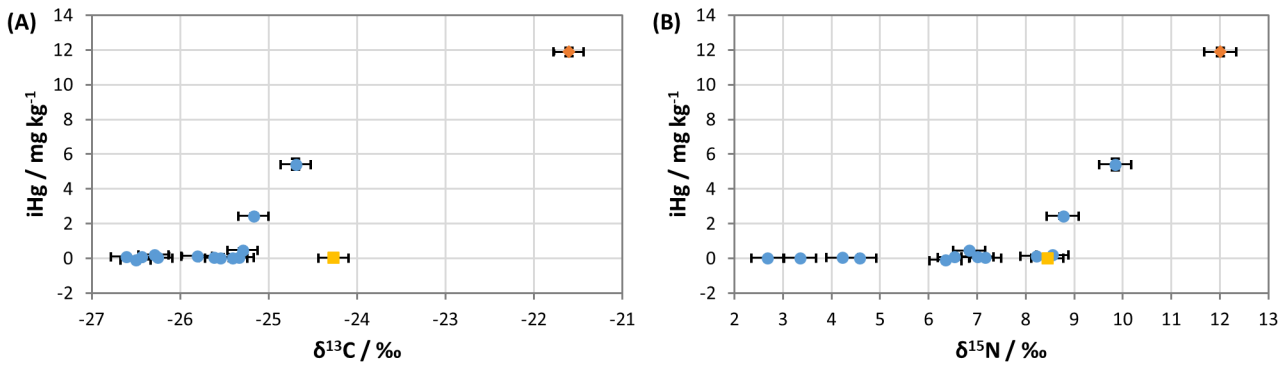

Figure 2 Comparison between iHg concentrations and carbon (A) and nitrogen (B) stable isotope ratio data for golden eagle liver samples (n = 15). Error bars represent 1σ. The highlighted 'outlier' samples (orange and yellow) originate from the Isle of Rum, Scotland, UK (and are discussed further below).

3.3. MeHg fraction differences in golden eagle livers

The T-Hg concentrations in golden eagle livers were plotted against MeHg fraction data in Figure 3. Though all sample concentrations obtained were above the limit of detection (LOD) for each analysis, three samples had MeHg concentrations below the limit of quantification (LOQ). Therefore, since the error on these results would be high, these data points were omitted from the graph. The results showed that as T-Hg increased, a decrease in the MeHg fraction occurred (regression ANOVA; $p = 0.021$).

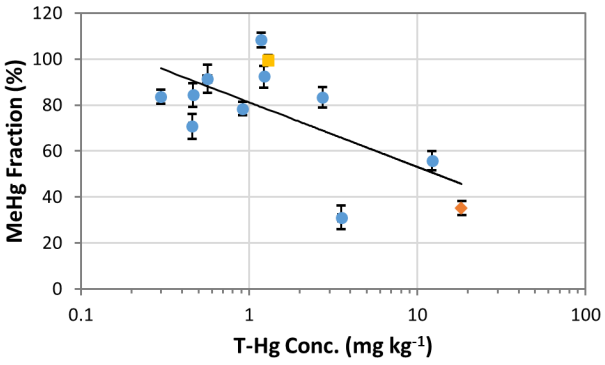

Figure 3 Variation in MeHg fraction with T-Hg concentration (log scale) in golden eagle liver tissue samples (n = 12). Error bars presented represent 1σ. Samples highlighted in orange and yellow are the two 'outlier' samples noted in Figure 2.

3.4. Comparison of iHg to T-Se in golden eagle livers

Given its previously documented potential to bind to iHg in the livers of cetaceans (Bolea-Fernandez et al., 2019; Gajdosechova et al., 2016) and, recently, seabirds (Manceau et al., 2021b; Renedo et al., 2021), T-Se concentrations in golden eagle liver samples were compared with iHg (Figure 4).

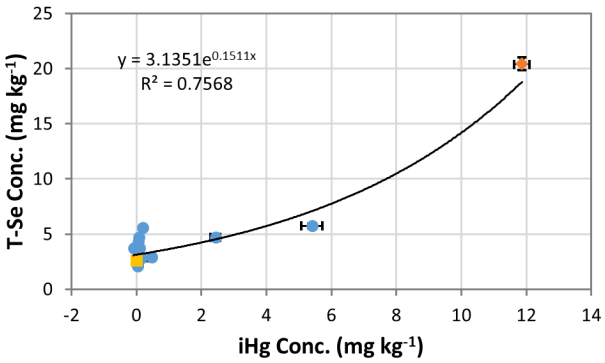

Figure 4 iHg concentration plotted against T-Se concentration in golden eagle livers (n = 15). Error bars presented represent 1σ. Samples highlighted in orange and yellow are the two 'outlier' samples noted in Figure 2.

The golden eagle with the highest iHg (11.9 mg kg^{-1}) also had extremely high T-Se (20.4 mg kg^{-1}) and can be treated as an obvious outlier. When this specimen is excluded, the T-Se concentration for all other samples follows a normal distribution ($p > 0.150$).

Calculated measurement uncertainty for a typical analysis of Se in the raptor livers showed a relative expanded uncertainty of 19.2%, much higher than that for MeHg or T-Hg measurements primarily due to the larger error in the certified value of T-Se in DOLT-4 (Table A.4b).

3.5. Analysis for the presence of Hg and Se nanoparticles in golden eagle livers

The three birds with the most elevated iHg concentrations (all >2 mg kg^{-1} on Figure 4), and the additional outlier for $\delta^{13}C$ (in yellow; Figure 3), which originated from the same location as the golden eagle with the highest iHg concentration (in orange; Figure 3), were subjected to sp-ICP-MS analysis to observe and quantify the presence of possible nanoparticles. Analysis of NIST RM 8013 gave a transport efficiency of 8.18%. Although the gold nanoparticles are likely different in terms of surface functionality to that of the biological nanoparticles, transport efficiency was assumed to be consistent between NIST RM 8013 and the Hg and Se measurements. The samples were diluted for analysis based on obtaining a final dilution of 0.5 ng mL^{-1} iHg. The limit of size detection of the method was found to be 17.6 nm (RSD = 1.3%). All four samples measured showed clear evidence of the presence of Hg

330 nanoparticles (Table A.5, Figure A.6). However the shape of the particle size distribution plots did not
331 approximate a normal distribution. Instead, the number of observed particles only increased as
332 particle size decreased towards the limit of size detection. This suggests that the true median particle
333 size likely lies below the limit of size detection in each case. The samples were also measured for Se,
334 which showed detectable nanoparticles (>25 nm). However, the number of detected particles were
335 too low (<1000) to obtain further reliable information.

336 To identify whether Hg and Se were co-located in hotspots within tissues (i.e., as nano or
337 microparticles), or, if these elements were homogeneously distributed within liver tissues, a thin
338 section of liver from the golden eagle outlier highlighted in orange in Figures 2–4 was analysed further
339 with LA-ICP-MS. This particular liver sample was chosen as it was the most extreme outlier for $\delta^{13}C$
340 and $\delta^{15}N$ and contained the highest iHg and T-Se content. Element maps, which give semi-quantitative
341 data, were then created for the thin section (Figure 5). The most abundant isotopes (^{80}Se and ^{202}Hg)
342 were used to obtain the best possible sensitivity, with hydrogen reaction gas additionally used to
343 remove the argon-based interference on ^{80}Se. Carbon intensities (Figure A.7) were used as an internal
344 standard to correct for instrumental drift and uneven sample thickness in order to ensure a normalised
345 comparison between the Hg and Se intensities across the liver sample. The maps displayed a clear
346 presence of Hg hotspots, which also correlated with hotspots of Se.

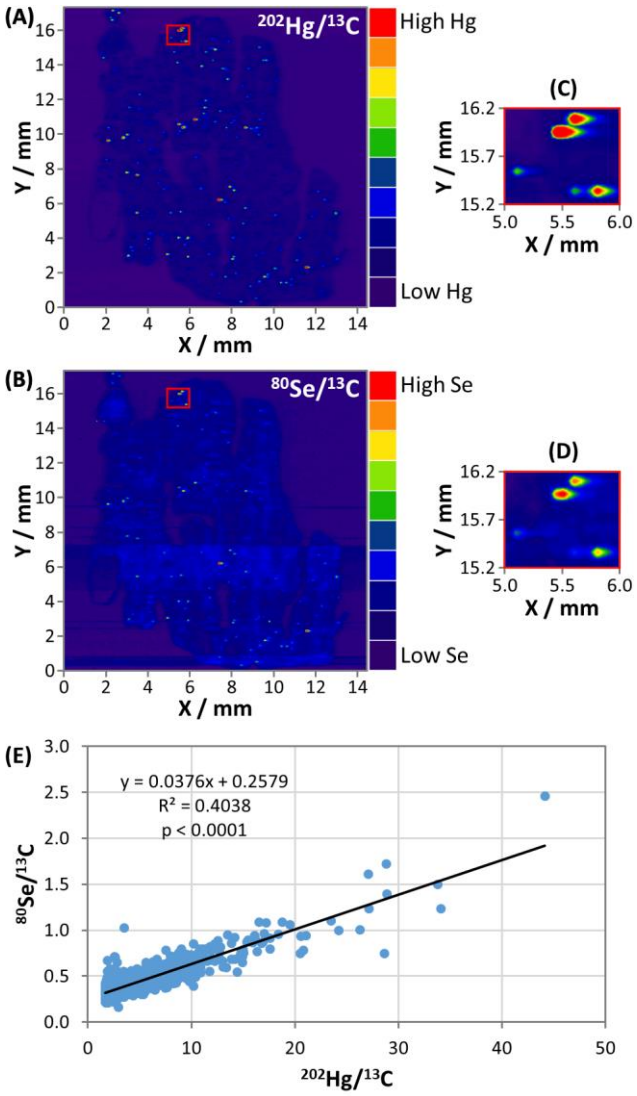

347

348 Figure 5 2D maps of ^{202}Hg/^{13}C (A) and ^{80}Se/^{13}C (B) in the liver of the golden eagle with the
349 highest observed iHg and high T-Se concentrations (highlighted orange; Figure 4).
350 Magnified sections of the ^{202}Hg/^{13}C and ^{80}Se/^{13}C plots are given in (C) and (D)
351 respectively. The scale displays intensity of the monitored isotope (in counts per
352 second), with low counts displaying in blue and high counts displaying in red.
353 Normalised Hg and Se counts (E) is also plotted.

354 Additional TEM imaging (n = 1) (Figure A.8) from the same golden eagle sample highlighted numerous
355 small dense materials, most likely nanoparticles. Size imaging assessment determined the particles to
356 range primarily between 10–20 nm in diameter.

4. Discussion

Most of the raptor liver samples tested here had concentrations (for both MeHg and T-Hg) within the 0–5 mg kg^{-1} dw range, however, some individuals showed much higher 'outlier' concentrations – up to approximately 24 mg kg^{-1} (Figure 1) for both MeHg and T-Hg in one hen harrier found on the Orkney isles in 2018 (Table A.1). Proposed liver Hg concentrations indicative of impaired reproduction and mortality are >2 mg kg^{-1} and >20 mg kg^{-1} wet weight (ww) respectively (Shore et al., 2011) (approximately equivalent to 7 mg kg^{-1} and 70 mg kg^{-1} dw in this study). Although no samples here exceeded the indicative concentration for mortality, 9 of the 117 raptor livers analysed showed Hg concentrations within the range of potential reproductive impairment, however no clear pattern was observed when considering location or sampling year. Of these 9 samples, one was an osprey (*Pandion haliaetus*), which typically would have a diet of fish and, thus, likely high MeHg. The other species include buzzards (n = 2), golden eagles (n = 2), hen harrier (n = 2), and sparrowhawk (n = 2), and their diets vary from carrion (insects, worms, small mammals) to larger mammals, birds, and sometimes fish. Some diet variation will exist between the prey items of individuals of the same species living inland to those living on the coast. For example, it is known that the diet of Scottish golden eagles consists primarily of lagamorphs (e.g. rabbits) and other mammals (Watson et al., 1993), however in the western isles their diet contains up to 20% of fish and waders/seabirds (Halley, 1998). Not all samples high in Hg were found in coastal locations, therefore there are likely also other potential dietary sources to consider.

Large variations in Hg concentrations were observed in buzzards, golden eagles, hen harriers, and sparrowhawks, spanning over two orders of magnitude. Similar large variations of Hg levels have previously been observed in a study on Norwegian birds of prey (Frøslie et al., 1986). The barn owls and tawny owls generally showed a smaller variation in Hg levels (when compared to the other species), and this could relate to a range of environmental, behavioural, or physiological factors. A similar study on Hg in raptors in Belgium showed that barn owls from a predominantly agricultural

area (n = 16) had 4 times higher Hg levels than barn owls from predominantly forest or meadow areas (n = 3) (Delbeke et al., 1984). Concentrations reported for T-Hg ranged from 0.07–4.31 mg kg^{-1} ww (equivalent to 0.24–14.8 mg kg^{-1} dw) in agricultural zones compared to 0.14–1.63 mg kg^{-1} ww (equivalent to 0.48–5.58 mg kg^{-1} dw) for meadow areas. The authors suggested that this difference in Hg was due to differing diets in the two areas. The concentration range of 0.22–1.19 mg kg^{-1} dw for barn owls observed in this study suggests a diet preference component closer to that of the birds foraging in meadow areas, likely small rodents rather than passerines. Similarly, tawny owls have a mostly rodent based diet, however, it also includes small birds, insects, amphibians, and earthworms (Taylor, 2016) potentially reflecting the slightly wider Hg concentration range when compared to the barn owl.

In terms of organic vs iHg speciation, most of the samples tested across all species had MeHg fractions between 80–120%, suggesting a low rate of demethylation of MeHg in these species or low uptake of iHg in diet. However, golden eagles statistically showed significantly lower MeHg fraction values, despite displaying statistically similar MeHg and T-Hg concentrations to sparrowhawks, buzzards, and hen harriers. Differences in behaviour and habit (i.e., prey selection) between these species may in part underlie these observations, and as such, stable isotope ratio data was collected here for golden eagles to consider if the differences in iHg values may correlate with isotopic indicators of diet (i.e., $\delta^{13}C$, $\delta^{15}N$ and $\delta^{34}S$ isotope ratios).

In terms of isotope data (Figure 2), we observed $\delta^{13}C$ values ranging from −27 to −23 ‰ with one specimen (highlighted in orange) with a value of −21.6 ‰. $\delta^{13}C$ values for terrestrial C_3 plants generally range from −32 ‰ to −23 ‰ (Kohn, 2010), which fits with the majority of the results observed in this study, except the outlier. The golden eagle livers displayed a wide variation in $\delta^{15}N$ values, ranging from approximately 2 to 12 ‰ overall. The wide range observed will likely depend on variations in the types of prey consumed. A terrestrial prey diet is ultimately affected by the plants (primary producers) in an area, which in turn are affected by: fertilisation and animal manure (where $\delta^{15}N$ is lowered by

mineral fertilisers but elevated by dung and seaweed fertilisation, causing changes of over 5 ‰ in plants) (Blanz et al., 2020, 2019; Bogaard et al., 2007; Fraser et al., 2011), soil salinity (van Groenigen and van Kessel, 2002), plant species and plant part (Cloern et al., 2002), rainfall (Handley et al., 1999), and temperature (Craine et al., 2009). Variations in these dietary factors is likely significant across the range of habitats occupied by Scottish golden eagles, hence the wide range of $\delta^{15}N$ values observed.

However, in three golden eagles with $\delta^{13}C$ values over −25.2 ‰, a notable increase in iHg with increasing (less negative) $\delta^{13}C$ values was observed. A similar increasing iHg concentration is also observed with increasing $\delta^{15}N$ values above 8.77 ‰. This suggests an additional dietary source with higher Hg levels and higher $\delta^{13}C$ and $\delta^{15}N$ values. However, the trends observed support previous knowledge of consumption of components of marine origin in the diets of birds from the Scottish Outer and Inner Hebrides (i.e., fulmars, gulls, waders, or pipits) (Watson et al., 1993, 1992). Carcasses of animals such as northern fulmar can have $\delta^{13}C$ values (in muscle) in the range of approximately −18 to −15 ‰ (Thompson and Furness, 1995) Alternatively, terrestrial C_4 plants, such as maize and millet, have $\delta^{13}C$ values around −16 to −10 ‰ (Basu et al., 2015; O'Leary, 1998) However, these plants are not present in significant quantities in Scotland (Rural and Environment Science and Analytical Services, 2019) or the wider British Isles and since Scottish golden eagles are not known to migrate or disperse out of the British Isles, apparently residing within the British Isles all of their lives (Watson, 2010), consumption of prey from regions where C_4 plants are common is unlikely. In addition, the more elevated $\delta^{15}N$ values alongside high iHg (Figure 2B) may also indicate a marine-influenced diet due to the higher trophic level implied. Therefore, given this evidence, for golden eagle livers with the most elevated $\delta^{13}C$ and $\delta^{15}N$ values, marine-influenced foods were likely consumed. Marine organisms are known to have elevated Hg concentrations around 0.03–3.2 mg kg^{-1} depending on trophic level (Mathieson and McLusky, 1995; Nigro and Leonzio, 1996). Scottish seabirds, such as northern fulmar, also show elevated Hg levels generally from 0.1–1.8 mg kg^{-1} dw (all tissues) (Thompson et al., 1990). Therefore, the increased proportion of iHg observed in the three golden eagle livers with rather elevated $\delta^{13}C$ and $\delta^{15}N$ values could be due to marine contributions to an otherwise largely terrestrial

diet. Hg intake from a marine diet is considered to be predominantly MeHg, which has a 100% uptake rate through the GI tract (Gochfeld, 2003) and, on average, makes up most of the T-Hg in muscle tissues of marine mammals (Wagemann et al., 1997). Dietary MeHg may undergo demethylation and deposit in the liver as one potential detoxification mechanism. Alternatively, other tissues of marine predators, such as the liver, may however contain lower MeHg fractions (Wagemann et al., 1997) and may be a potential source of dietary iHg.

No trend was observed for any form of Hg with the $\delta^{34}S$ values, which ranged from 12 to 20 ‰. Sulphate from terrestrial and aquatic environments show $\delta^{34}S$ values generally within −2 to 9 ‰ (Alling et al., 2008; Croisetière et al., 2009), whereas marine sulphate shows $\delta^{34}S$ values of approximately 21 ‰ (Rees et al., 1978). This may suggest that all the golden eagles here were (at least partly) marine foraging, which does not agree with the $\delta^{13}C$ or $\delta^{15}N$ ratios, or, known common golden eagle feeding behaviour across Scotland. Instead, it may be that other effects, such as the effect of sea spray (shown recently (Guiry and Szpak, 2020)) may mask dietary influences. Therefore, the $\delta^{34}S$ values here were not considered further.

One outlier, presented in yellow on these graphs (i.e., Figure 2A) had low iHg but a slightly elevated $\delta^{13}C$ value. This sample, as well as the specimen with the highest iHg concentration and highest $\delta^{13}C$ value (orange), originated from the Isle of Rum. The outlier highlighted in yellow cannot be fully explained by a high consumption of seabirds, such as fulmar, as it is not an outlier for $\delta^{15}N$, which would be expected since fulmar have $\delta^{15}N$ values in the range of 13 to 15 ‰ (Thompson and Furness, 1995). A study conducted on the red deer present on Rum (n = 54) found that $\delta^{13}C$ values here were generally higher (up to 1 ‰) in these deer than in those from other Scottish regions (Stevens et al., 2006). This study suggested that this was a result of consumption of seaweed, which has been previously observed as a contribution to their diet (Conradt, 2000). These two outlier eagles may have scavenged upon these deer, and therefore, this could account, at least in part, for the elevated $\delta^{13}C$ values seen.

458 iHg tends to bind with Se in the liver of animals (Cuvin-Aralar and Furness, 1991). In order to determine
459 if this was indeed the case here, laser ablation imaging of a liver thin section from one golden eagle
460 with the most extreme iHg level was carried out. Figure 5 confirms that not only is this true in this
461 case, but that the Se and Hg can be found as micro or nanoparticles in the liver. Due to the resolution
462 of our laser ablation approach, the size of these particles could not be accurately determined. Further
463 analysis of the same golden eagle liver by TEM measurements (Figure A.8) demonstrated the likely
464 presence of nanoparticles ranging primarily between 10–20 nm in diameter. Subsequently, four
465 golden eagles tested for nanoparticles by sp-ICP-MS showed definitively that Hg nanoparticles were
466 present in the range of <18–43 nm, with the number of particles present scaling in magnitude
467 relatively with the iHg concentration. Se nanoparticles were detected, but the particle numbers
468 observed were too low to draw firm conclusions by this method, which could be due to the enzymatic
469 digestion changing the nanoparticle characteristic (e.g. by dissolution of a selenoprotein corona),
470 which was not studied further here. However, the combination of all the data clearly demonstrates
471 the occurrence of Hg nanoparticles co-locating with Se in the liver of golden eagles, likely as HgSe
472 nanoparticles.

473 The presence of these nanoparticles in the liver could be interpreted by two possible hypotheses;
474 either these golden eagles are able to form these nanoparticles through demethylation of MeHg, or
475 these nanoparticles could have been taken up through their diet – especially given that similar
476 nanoparticles have previously been observed in cetaceans (Bolea-Fernandez et al., 2019;
477 Gajdosechova et al., 2016), a food item that eagles from Rum (for example) could periodically have
478 access to (due to carcass stranding). If demethylation is occurring, a decrease in MeHg fraction with
479 increasing T-Hg should be observed. This trend has been observed in this study (Figure 3), which may
480 suggest that active demethylation of MeHg is taking place in the liver of the golden eagles as total
481 levels increase. This method of MeHg detoxification is known to occur in other bird species, such as
482 waterbirds and common loons (Eagles-Smith et al., 2009b), however, the T-Hg threshold
483 concentration above which demethylation occurs (of 8.5 mg kg^{-1}, as observed previously) may actually

484 be much lower given the data from this study. This, combined with the statistically similar
485 concentration ranges of MeHg and T-Hg to that of sparrowhawks, hen harriers, and buzzards, may
486 suggest that some golden eagles are especially good at demethylation and mineralisation to form
487 these HgSe nanoparticles, possibly as described recently for seabirds (Manceau et al., 2021b), as a
488 detoxification mechanism at a low T-Hg threshold, in addition to detoxification by other routes, such
489 as faecal excretion or excretion to feathers (Lewis and Furness, 1991).

490 Binding of Hg to Se may reduce circulating essential Se levels in the body, promoting increased
491 accumulation of Se to compensate (given Se is essential to form important selenoproteins). Previous
492 studies of Hg in birds do indeed show a trend of increasing Se concentrations with Hg concentrations
493 (Henny et al., 2002). However, the trend seen in Figure 4 (which admittedly relies on only three
494 samples with elevated iHg concentrations and one sample with very high Se concentration) may not
495 show this behaviour. If the most extreme specimen is omitted, then the other samples tested fall into
496 a normal Se distribution, suggesting that all other samples reflect a normal background level of Se.
497 This outlier sample also showed elevated iHg but not elevated MeHg when compared to the other
498 two outlier samples with iHg between 2–6 mg kg^{-1}.

499 Although the formation of HgSe nanoparticles has previously been confirmed in cetaceans and
500 seabirds, to our knowledge, it has not yet been shown that demethylation of MeHg forms similar
501 nanoparticles in terrestrial birds of prey, who typically have a far lower dietary MeHg intake. Though
502 this study contains too few samples to draw firm conclusions as to the source of these nanoparticles,
503 the evidence presented (from stable isotope analysis and our other data) may suggest that the
504 presence of these particles found in some golden eagles could be due to a marine-influenced diet. This
505 study highlights the importance of considering not only broad 'trends' in data relevant to
506 ecotoxicology – but also in exploring the nature of outliers in datasets, which can provide intriguing
507 insights regarding the fate and behaviour of Hg in the food chains of these top predators. Looking
508 ahead, it would be beneficial to understand if these observations are unique to these individuals or

indicative of a more common phenomenon (i.e., detoxification mechanism) in certain avian species through further investigation with a larger sample set.

Author contributions

Shaun T. Lancaster: Performed the measurements of T-Hg, MeHg, T-Se, and sp-ICP-MS. Performed statistical interpretations of results. Lead author of the submitted manuscript. **Gabriela Peniche:** Sample collection and dissection. Provided input on ecological interpretations of results. **Ali Alzahrani:** Performed the nanoparticle analysis by LA-ICP-MS and TEM. **Magdalena Blanz:** Provided input on the interpretation of stable isotope ratios. **Jason Newton:** Performed the analysis of stable isotope ratios. **Mark A. Taggart:** Conceptualisation, supervision, and editing. **Warren T. Corns:** Supervision, and editing. **Eva M. Krupp:** Conceptualisation, supervision, and editing. **Jörg Feldmann:** Conceptualisation, supervision, and editing.

Conflicts of interest

There are no conflicts to declare.

Acknowledgements

S. Lancaster would like to thank PS Analytical for funding and support for the project. G. Peniche was funded under a NERC CASE studentship agreement (University of Edinburgh – SNH – SASA). The authors gratefully acknowledge the Microscopy and Histology Core Facility at the Institute for Medical Sciences, Aberdeen for their support & assistance in this work.

References

Ackerman, J.T., Herzog, M.P., Evers, D.C., Cristol, D.A., Kenow, K.P., Heinz, G.H., Lavoie, R.A., Brasso, R.L., Mallory, M.L., Provencher, J.F., Braune, B.M., Matz, A., Schmutz, J.A., Eagles-Smith, C.A., Savoy, L.J., Meyer, M.W., Hartman, C.A., 2020. Synthesis of Maternal Transfer of Mercury in Birds: Implications for Altered Toxicity Risk. Environ. Sci. Technol. 54, 2878–2891. https://doi.org/10.1021/acs.est.9b06119

533 Alling, V., Humborg, C., Mörth, C.M., Rahm, L., Pollehne, F., 2008. Tracing terrestrial organic matter
534 by δ34S and δ13C signatures in a subarctic estuary. Limnol. Oceanogr. 53, 2594–2602.
535 https://doi.org/10.4319/lo.2008.53.6.2594

536 Barwick, V.J., Ellison, S.L.R., 1999. Measurement uncertainty: Approaches to the evaluation of
537 uncertainties associated with recovery. Analyst 124, 981–990.
538 https://doi.org/10.1039/a901845j

539 Basu, S., Agrawal, S., Sanyal, P., Mahato, P., Kumar, S., Sarkar, A., 2015. Carbon isotopic ratios of
540 modern C3–C4 plants from the Gangetic Plain, India and its implications to paleovegetational
541 reconstruction. Palaeogeogr. Palaeoclimatol. Palaeoecol. 440, 22–32.
542 https://doi.org/10.1016/j.palaeo.2015.08.012

543 Bearhop, S., Ruxton, G.D., Furness, R.W., 2000. Dynamics of mercury in blood and feathers of great
544 skuas. Environ. Toxicol. Chem. 19, 1638–1643. https://doi.org/10.1002/etc.5620190622

545 Becker, J.S., Matusch, A., Wu, B., 2014. Bioimaging mass spectrometry of trace elements – recent
546 advance and applications of LA-ICP-MS: A review. Anal. Chim. Acta 835, 1–18.
547 https://doi.org/10.1016/j.aca.2014.04.048

548 Blanz, M., Ascough, P., Mainland, I., Martin, P., Taggart, M.A., Dieterich, B., Wishart, J., Sayle, K.L.,
549 Raab, A., Feldmann, J., 2019. Seaweed fertilisation impacts the chemical and isotopic
550 composition of barley: Implications for analyses of archaeological skeletal remains. J. Archaeol.
551 Sci. 104, 34–44. https://doi.org/10.1016/j.jas.2019.02.003

552 Blanz, M., Mainland, I., Richards, M., Balasse, M., Ascough, P., Wolfhagen, J., Taggart, M.A.,
553 Feldmann, J., 2020. Identifying seaweed consumption by sheep using isotope analysis of their
554 bones and teeth: Modern reference δ13C and δ15N values and their archaeological
555 implications. J. Archaeol. Sci. 118. https://doi.org/10.1016/j.jas.2020.105140

556 Bogaard, A., Heaton, T.H.E., Poulton, P., Merbach, I., 2007. The impact of manuring on nitrogen

isotope ratios in cereals: archaeological implications for reconstruction of diet and crop management practices. J. Archaeol. Sci. 34, 335–343. https://doi.org/10.1016/j.jas.2006.04.009

Bolea-Fernandez, E., Rua-Ibarz, A., Krupp, E.M., Feldmann, J., Vanhaecke, F., 2019. High-precision isotopic analysis sheds new light on mercury metabolism in long-finned pilot whales (Globicephala melas). Sci. Rep. 9, 1–10. https://doi.org/10.1038/s41598-019-43825-z

Bouland, A.J., White, A.E., Lonabaugh, K.P., Varian-Ramos, C.W., Cristol, D.A., 2012. Female-biased offspring sex ratios in birds at a mercury-contaminated river. J. Avian Biol. 43, 244–251. https://doi.org/10.1111/j.1600-048X.2012.05612.x

Carlson, J.R., Cristol, D., Swaddle, J.P., 2014. Dietary mercury exposure causes decreased escape takeoff flight performance and increased molt rate in European starlings (Sturnus vulgaris). Ecotoxicology 23, 1464–1473. https://doi.org/10.1007/s10646-014-1288-5

Cherel, Y., Hobson, K.A., Hassani, S., 2005. Isotopic discrimination between food and blood and feathers of captive penguins: Implications for dietary studies in the wild. Physiol. Biochem. Zool. 78, 106–115. https://doi.org/10.1086/425202

Chételat, J., Ackerman, J.T., Eagles-Smith, C.A., Hebert, C.E., 2020. Methylmercury exposure in wildlife: A review of the ecological and physiological processes affecting contaminant concentrations and their interpretation. Sci. Total Environ. 711. https://doi.org/10.1016/j.scitotenv.2019.135117

Chisholm, B.S., Nelson, D.E., Schwarcz, H.P., 1982. Stable-Carbon Isotope Ratios as a Measure of Marine Versus Terrestrial Protein in Ancient Diets. Science (80-.). 216, 1131–1133. https://doi.org/10.1126/science.216.4550.1131

Cloern, J.E., Canuel, E.A., Harris, D., 2002. Stable carbon and nitrogen isotope composition of aquatic and terrestrial plants of the San Francisco Bay estuarine system. Limnol. Oceanogr. 47, 713–729. https://doi.org/10.4319/lo.2002.47.3.0713

581 Conradt, L., 2000. Use of a seaweed habitat by red deer (Cervus elaphus L.). J. Zool. London 250,
582 541–549. https://doi.org/10.1111/j.1469-7998.2000.tb00795.x

583 Coplen, T.B., Brand, W.A., Gehre, M., Gröning, M., Meijer, H.A.J., Toman, B., Verkouteren, R.M.,
584 2006. New guidelines for δ13C measurements. Anal. Chem. 78, 2439–2441.
585 https://doi.org/10.1021/ac052027c

586 Craine, J.M., Elmore, A.J., Aidar, M.P.M., Bustamante, M., Dawson, T.E., Hobbie, E.A., Kahmen, A.,
587 MacK, M.C., McLauchlan, K.K., Michelsen, A., Nardoto, G.B., Pardo, L.H., Peñuelas, J., Reich,
588 P.B., Schuur, E.A.G., Stock, W.D., Templer, P.H., Virginia, R.A., Welker, J.M., Wright, I.J., 2009.
589 Global patterns of foliar nitrogen isotopes and their relationships with climate, mycorrhizal
590 fungi, foliar nutrient concentrations, and nitrogen availability. New Phytol. 183, 980–992.
591 https://doi.org/10.1111/j.1469-8137.2009.02917.x

592 Cristol, D.A., Brasso, R.L., Condon, A.M., Fovargue, R.E., Friedman, S.L., Hallinger, K.K., Monroe, A.P.,
593 White, A.E., 2008. The movement of aquatic mercury through terrestrial food webs. Science
594 (80-.). 320, 335. https://doi.org/10.1126/science.1154082

595 Croisetière, L., Hare, L., Tessier, A., Cabana, G., 2009. Sulphur stable isotopes can distinguish trophic
596 dependence on sediments and plankton in boreal lakes. Freshw. Biol. 54, 1006–1015.
597 https://doi.org/10.1111/j.1365-2427.2008.02147.x

598 Cuvin-Aralar, M.L.A., Furness, R.W., 1991. Mercury and selenium interaction: A review. Ecotoxicol.
599 Environ. Saf. 21, 348–364. https://doi.org/10.1016/0147-6513(91)90074-Y

600 Day, R.D., Christopher, S.J., Becker, P.R., Whitaker, D.W., 2005. Monitoring mercury in the
601 loggerhead sea turtle, Caretta caretta. Environ. Sci. Technol. 39, 437–446.
602 https://doi.org/10.1021/es049628q

603 Delbeke, K., Joiris, C., Decadtt, G., 1984. Mercury Contamination of the Belgian Avifauna 1970–1981.
604 Environ. Pollut. Ser. B 7, 205–221. https://doi.org/10.1016/0143-148X(84)90049-1

605 Eagles-Smith, C.A., Ackerman, J.T., De La Cruz, S.E.W., Takekawa, J.Y., 2009a. Mercury
606 bioaccumulation and risk to three waterbird foraging guilds is influenced by foraging ecology
607 and breeding stage. Environ. Pollut. 157, 1993–2002.
608 https://doi.org/10.1016/j.envpol.2009.03.030

609 Eagles-Smith, C.A., Ackerman, J.T., Julie, Y.E.E., Adelsbach, T.L., 2009b. Mercury demethylation in
610 waterbird livers: Dose-response thresholds and differences among species. Environ. Toxicol.
611 Chem. 28, 568–577. https://doi.org/10.1897/08-245.1

612 Ellison, S.L.R., Williams, A. (Eds.), 2012. Eurachem/CITAC guide: Quantifying Uncertainty in Analytical
613 Measurements, 3rd Edit. ed, Eurachem/CITAC guide.

614 Evers, D.C., Savoy, L.J., Desorbo, C.R., Yates, D.E., Hanson, W., Taylor, K.M., Siegel, L.S., Cooley, J.H.,
615 Bank, M.S., Major, A., Munney, K., Mower, B.F., Vogel, H.S., Schoch, N., Pokras, M., Goodale,
616 M.W., Fair, J., 2008. Adverse effects from environmental mercury loads on breeding common
617 loons. Ecotoxicology 17, 69–81. https://doi.org/10.1007/s10646-007-0168-7

618 Fraser, R.A., Bogaard, A., Heaton, T., Charles, M., Jones, G., Christensen, B.T., Halstead, P., Merbach,
619 I., Poulton, P.R., Sparkes, D., Styring, A.K., 2011. Manuring and stable nitrogen isotope ratios in
620 cereals and pulses: Towards a new archaeobotanical approach to the inference of land use and
621 dietary practices. J. Archaeol. Sci. 38, 2790–2804. https://doi.org/10.1016/j.jas.2011.06.024

622 Frøslie, A., Holt, G., Norheim, G., 1986. Mercury and persistent chlorinated hydrocarbons in owls
623 Strigiformes and birds of prey Falconiformes collected in Norway during the period 1965-1983.
624 Environ. Pollution. Ser. B, Chem. Phys. 11, 91–108. https://doi.org/10.1016/0143-
625 148X(86)90037-6

626 Gajdosechova, Z., Lawan, M.M., Urgast, D.S., Raab, A., Scheckel, K.G., Lombi, E., Kopittke, P.M.,
627 Loeschner, K., Larsen, E.H., Woods, G., Brownlow, A., Read, F.L., Feldmann, J., Krupp, E.M.,
628 2016. In vivo formation of natural HgSe nanoparticles in the liver and brain of pilot whales. Sci.

629 Rep. 6, 1–11. https://doi.org/10.1038/srep34361

630 Gochfeld, M., 2003. Cases of mercury exposure, bioavailability, and absorption. Ecotoxicol. Environ.
631 Saf. 56, 174–179. https://doi.org/10.1016/S0147-6513(03)00060-5

632 González, A.G., Herrador, M.Á., 2007. The assessment of electronic balances for accuracy of mass
633 measurements in the analytical laboratory. Accredit. Qual. Assur. 12, 21–29.
634 https://doi.org/10.1007/s00769-006-0214-9

635 Guiry, E.J., Szpak, P., 2020. Seaweed-eating sheep show that δ34S evidence for marine diets can be
636 fully masked by sea spray effects. Rapid Commun. Mass Spectrom. e8868.
637 https://doi.org/10.1002/rcm.8868

638 Halley, D.J., 1998. Golden and White-tailed Eagle in Scotland and Norway: co-existence, competition
639 and environmental degradation. Br. Birds 91, 171–179.

640 Handley, L.L., Austin, A.T., Robinson, D., Scrimgeour, C.M., Raven, J.A., Heaton, T.H.E., Schmidt, S.,
641 Stewart, G.R., 1999. The 15N natural abundance (δ15N) of ecosystem samples reflects
642 measures of water availability. Aust. J. Plant Physiol. 26, 185–199.
643 https://doi.org/10.1071/PP98146

644 Hebert, C.E., Bur, M., Sherman, D., Shutt, J.L., 2008. Sulfur isotopes link overwinter habitat use and
645 breeding condition in double-crested cormorants. Ecol. Appl. 18, 561–567.
646 https://doi.org/10.1890/07-1278.1

647 Henny, C.J., Hill, E.F., Hoffman, D.J., Spalding, M.G., Grove, R.A., 2002. Nineteenth century mercury:
648 Hazard to wading birds and cormorants of the Carson River, Nevada. Ecotoxicology 11, 213–
649 231. https://doi.org/10.1023/A:1016327602656

650 Hobson, K.A., Clark, R.G., 1992. Assessing avian diets using stable isotopes II: factors influencing diet-
651 tissue fractionation. Condor 94, 189–197. https://doi.org/10.2307/1368808

652 Inger, R., Bearhop, S., 2008. Applications of stable isotope analyses to avian ecology. Ibis (Lond.
653 1859). 150, 447–461. https://doi.org/10.1111/j.1474-919X.2008.00839.x

654 JCGM 100:2008, 2008. Evaluation of measurement data — Guide to the expression of uncertainty in
655 measurement, International Organization for Standardization Geneva ISBN.

656 Kadis, R., 2017. Evaluation of the measurement uncertainty: Some common mistakes with a focus on
657 the uncertainty from linear calibration. J. Chromatogr. A 1499, 226–229.
658 https://doi.org/10.1016/j.chroma.2017.03.078

659 Kelly, J.F., 2000. Stable isotopes of carbon and nitrogen in the study of avian and mammalian trophic
660 ecology. Can. J. Zool. 78, 1–27. https://doi.org/10.1139/z99-165

661 Kenow, K.P., Meyer, M.W., Hines, R.K., Karasov, W.H., 2007. Distribution and Accumulation of
662 Mercury in Tissues of Captive-Reared Common Loon (Gavia Immer) Chicks. Environ. Toxicol.
663 Chem. 26, 1047–1055.

664 Kohn, M.J., 2010. Carbon isotope compositions of terrestrial C3 plants as indicators of (paleo)ecology
665 and (paleo)climate. Proc. Natl. Acad. Sci. 107, 19691–19695.
666 https://doi.org/10.1073/pnas.1004933107

667 Lancaster, S.T., Brombach, C.C., Corns, W.T., Feldmann, J., Krupp, E.M., 2019. Determination of
668 methylmercury using liquid chromatography-photochemical vapour generation-atomic
669 fluorescence spectroscopy (LC-PVG-AFS): A simple, green analytical method. J. Anal. At.
670 Spectrom. 34, 1166–1172. https://doi.org/10.1039/c9ja00037b

671 Lewis, S.A., Furness, R.W., 1993. The role of eggs in mercury excretion by Quail Coturnix coturnix and
672 the implications for monitoring mercury pollution by analysis of feathers. Ecotoxicology 2, 55–
673 64.

674 Lewis, S.A., Furness, R.W., 1991. Mercury accumulation and excretion in laboratory reared black-
675 headed gull Larus ridibundus chicks. Arch. Environ. Contam. Toxicol. 21, 316–320.

https://doi.org/10.1007/BF01055352

Lurz, P.W.W., Krauze-Gryz, D., Gryz, J., Meredith, A., Schilling, A.-K., Thain, C., Heller, E., 2017. Invisible threats to native mammals – mercury levels in three Eurasian red squirrel populations. Hystrix, Ital. J. Mammal. 28, 280–283. https://doi.org/10.4404/hystrix–28.2-12335

Manceau, A., Bourdineaud, J.-P., Oliveira, R.B., Sarrazin, S.L.F., Krabbenhoft, D.P., Eagles-Smith, C.A., Ackerman, J.T., Stewart, A.R., Ward-Deitrich, C., Busto, M.E. del C., Goenaga-Infante, H., Wack, A., Retegan, M., Detlefs, B., Glatzel, P., Bustamante, P., Nagy, K.L., Poulin, B.A., 2021a. Demethylation of Methylmercury in Bird, Fish, and Earthworm. Environ. Sci. Technol. 55, 1527–1534. https://doi.org/10.1021/acs.est.0c04948

Manceau, A., Gaillot, A.C., Glatzel, P., Cherel, Y., Bustamante, P., 2021b. In Vivo Formation of HgSe Nanoparticles and Hg-Tetraselenolate Complex from Methylmercury in Seabirds-Implications for the Hg-Se Antagonism. Environ. Sci. Technol. 55, 1515–1526. https://doi.org/10.1021/acs.est.0c06269

Mathieson, S., McLusky, D.S., 1995. Inter-species variation of mercury in skeletal muscle of five fish species from inshore waters of the Firth of Clyde, Scotland. Mar. Pollut. Bull. 30, 283–286. https://doi.org/10.1016/0025-326X(95)00047-Q

McKinney, C.R., McCrea, J.M., Epstein, S., Allen, H.A., Urey, H.C., 1950. Improvements in mass spectrometers for the measurement of small differences in isotope abundance ratios. Rev. Sci. Instrum. 21, 724–730. https://doi.org/10.1063/1.1745698

Meermann, B., Nischwitz, V., 2018. ICP-MS for the analysis at the nanoscale – a tutorial review. J. Anal. At. Spectrom. 33, 1432–1468. https://doi.org/10.1039/C8JA00037A

Mergler, D., Anderson, H.A., Hing Man Chang, L., Mahaffey, K.R., Murray, M., Sakamoto, M., Stern, A.H., 2007. Methylmercury Exposure and Health Effects in Humans: A Worldwide Concern. Ambio 36, 3–11. https://doi.org/10.1579/0044-7447(2007)36[3:MEAHEI]2.0.CO;2

700 Monteiro, L.R., Furness, R.W., 2001. Kinetics, dose-response, and excretion of methylmercury in
701 free-living adult Cory's shearwaters. Environ. Sci. Technol. 35, 739–746.
702 https://doi.org/10.1021/es000114a

703 Nigro, M., Leonzio, C., 1996. Intracellular storage of mercury and selenium in different marine
704 vertebrates. Mar. Ecol. Prog. Ser. 135, 137–143. https://doi.org/10.3354/meps135137

705 O'Leary, M.H., 1998. Carbon Isotopes in Photosynthesis. Bioscience 38, 328–336.
706 https://doi.org/10.2307/1310735

707 Obrist, D., Kirk, J.L., Zhang, L., Sunderland, E.M., Jiskra, M., Selin, N.E., 2018. A review of global
708 environmental mercury processes in response to human and natural perturbations: Changes of
709 emissions, climate, and land use. Ambio 47, 116–140. https://doi.org/10.1007/s13280-017-
710 1004-9

711 Palma, L., Beja, P., Tavares, P.C., Monteiro, L.R., 2005. Spatial variation of mercury levels in nesting
712 Bonelli's eagles from Southwest Portugal: effects of diet composition and prey contamination.
713 Environ. Pollut. 134, 549–557. https://doi.org/10.1016/j.envpol.2004.05.017

714 Qi, H., Coplen, T.B., Geilmann, H., Brand, W.A., Böhlke, J.K., 2003. Two new organic reference
715 materials for δ13C and δ15N measurements and a new value for the δ13C of NBS 22 oil. Rapid
716 Commun. Mass Spectrom. 17, 2483–2487. https://doi.org/10.1002/rcm.1219

717 Rauwel, P., Küünal, S., Ferdov, S., Rauwel, E., 2015. A Review on the Green Synthesis of Silver
718 Nanoparticles and Their Morphologies Studied via TEM. Adv. Mater. Sci. Eng. 2015, 682749.
719 https://doi.org/10.1155/2015/682749

720 Rees, C.E., Jenkins, W.J., Monster, J., 1978. The sulphur isotopic composition of ocean water
721 sulphate. Geochim. Cosmochim. Acta 42, 377–381. https://doi.org/10.1016/0016-
722 7037(78)90268-5

723 Renedo, M., Pedrero, Z., Amouroux, D., Cherel, Y., Bustamante, P., 2021. Mercury isotopes of key

724 tissues document mercury metabolic processes in seabirds. Chemosphere 263, 127777.
725 https://doi.org/10.1016/j.chemosphere.2020.127777

726 Rural and Environment Science and Analytical Services, 2019. Scottish Agricultural Census: June
727 2019.

728 Scheuhammer, A.M., Meyer, M.W., Sandheinrich, M.B., Murray, M.W., 2007. Effects of
729 environmental methylmercury on the health of wild birds, mammals, and fish. Ambio 36, 12–
730 18. https://doi.org/10.1579/0044-7447(2007)36[12:EOEMOT]2.0.CO;2

731 Scheuhammer, A.M., Wong, A.H.K., Bond, D., 1998. Mercury and selenium accumulation in common
732 loons (Gavia immer) and common mergansers (Mergus merganser) from Eastern Canada.
733 Environ. Toxicol. Chem. 17, 197–201. https://doi.org/10.1897/1551-
734 5028(1998)017<0197:MASAIC>2.3.CO;2

735 Schoeninger, M.J., DeNiro, M.J., 1984. Nitrogen and carbon isotopic composition of bone collagen
736 from marine and terrestrial animals. Geochim. Cosmochim. Acta 48, 625–639.
737 https://doi.org/10.1016/0016-7037(84)90091-7

738 Seewagen, C.L., Ma, Y., Morbey, Y.E., Guglielmo, C.G., 2019. Stopover departure behavior and flight
739 orientation of spring-migrant Yellow-rumped Warblers (Setophaga coronata) experimentally
740 exposed to methylmercury. J. Ornithol. 160, 617–624. https://doi.org/10.1007/s10336-019-
741 01641-2

742 Shore, R.F., Pereira, M.G., Walker, L.A., Thompson, D.R., 2011. Mercury in Non-marine Birds and
743 Mammals, in: Beyer, W.N., Meador, J.P. (Eds.), Environmental Contaminants in Biota:
744 Interpreting Tissue Concentrations. CRC Press, Boca Raton, FL.

745 Skinner, C., Mill, A.C., Newman, S.P., Newton, J., Cobain, M.R.D., Polunin, N.V.C., 2019. Novel tri-
746 isotope ellipsoid approach reveals dietary variation in sympatric predators. Ecol. Evol. 9,
747 13267–13277. https://doi.org/10.1002/ece3.5779

748 Stevens, R.E., Lister, A.M., Hedges, R.E.M., 2006. Predicting diet, trophic level and palaeoecology
749 from bone stable isotope analysis: a comparative study of five red deer populations. Oecologia
750 149, 12–21. https://doi.org/10.1007/s00442-006-0416-1

751 Syversen, T., Kaur, P., 2012. The toxicology of mercury and its compounds. J. Trace Elem. Med. Biol.
752 26, 215–226. https://doi.org/10.1016/j.jtemb.2012.02.004

753 Taylor, M., 2016. RSPB British Birds of Prey. Bloomsbury Publishing.

754 Thompson, D.R., Furness, R.W., 1995. Stable-Isotope Ratios of Carbon and Nitrogen in Feathers
755 Indicate Seasonal Dietary Shifts in Northern Fulmars. Auk 112, 493–498.
756 https://doi.org/10.2307/4088739

757 Thompson, D.R., Stewart, F.M., Furness, R.W., 1990. Using seabirds to monitor mercury in marine
758 environments. The validity of conversion ratios for tissue comparisons. Mar. Pollut. Bull. 21,
759 339–342. https://doi.org/10.1016/0025-326X(90)90795-A

760 UN Environment, 2019. Global Mercury Assessment 2018. UN Environ. Program. Chem. Heal. Branch
761 Geneva, Switz.

762 UN Environment, 2017. Minamata Convention on Mercury.

763 van Groenigen, J.-W., van Kessel, C., 2002. Salinity-induced Patterns of Natural Abundance Carbon-
764 13 and Nitrogen-15 in Plant and Soil. Soil Sci. Soc. Am. J. 66, 489–498.
765 https://doi.org/10.2136/sssaj2002.4890

766 Van Look, G., Meyer, V.R., 2002. The purity of laboratory chemicals with regard to measurement
767 uncertainty. Analyst 127, 825–829. https://doi.org/10.1039/b107958c

768 Wagemann, R., Trebacz, E., Hunt, R., Boila, G., 1997. Percent methylmercury and organic mercury in
769 tissues of marine mammals and fish using different experimental and calculation methods.
770 Environ. Toxicol. Chem. 16, 1859–1866. https://doi.org/10.1002/etc.5620160914

771 Watson, J., 2010. The Golden Eagle, Second Edi. ed. T&AD Poyser, London.

772 Watson, J., Leitch, A.F., Broad, R.A., 1992. The diet of the Sea Eagle Haliaeetus albicilla and Golden
773 Eagle Aquila chrysaetos in western Scotland. Ibis (Lond. 1859). 134, 27–31.
774 https://doi.org/10.1111/j.1474-919X.1992.tb07225.x

775 Watson, J., Leitch, A.F., Rae, S.R., 1993. The diet of Golden Eagles Aquila chrysaetos in Scotland. Ibis
776 (Lond. 1859). 135, 387–393. https://doi.org/10.1111/j.1474-919X.1993.tb02110.x

777 Werner, R.A., Brand, W.A., 2001. Referencing strategies and techniques in stable isotope ratio
778 analysis. Rapid Commun. Mass Spectrom. 15, 501–519. https://doi.org/10.1002/rcm.258

779 Zanden, M.J. Vander, Casselman, J.M., Rasmussen, J.B., 1999. Vander Zanden et al. 1999_ food web
780 consequences of species invasions in lakes. Nature 401, 1997–2000.

781

Figure 1

Click here to access/download;Figure;Figure 1.tiff

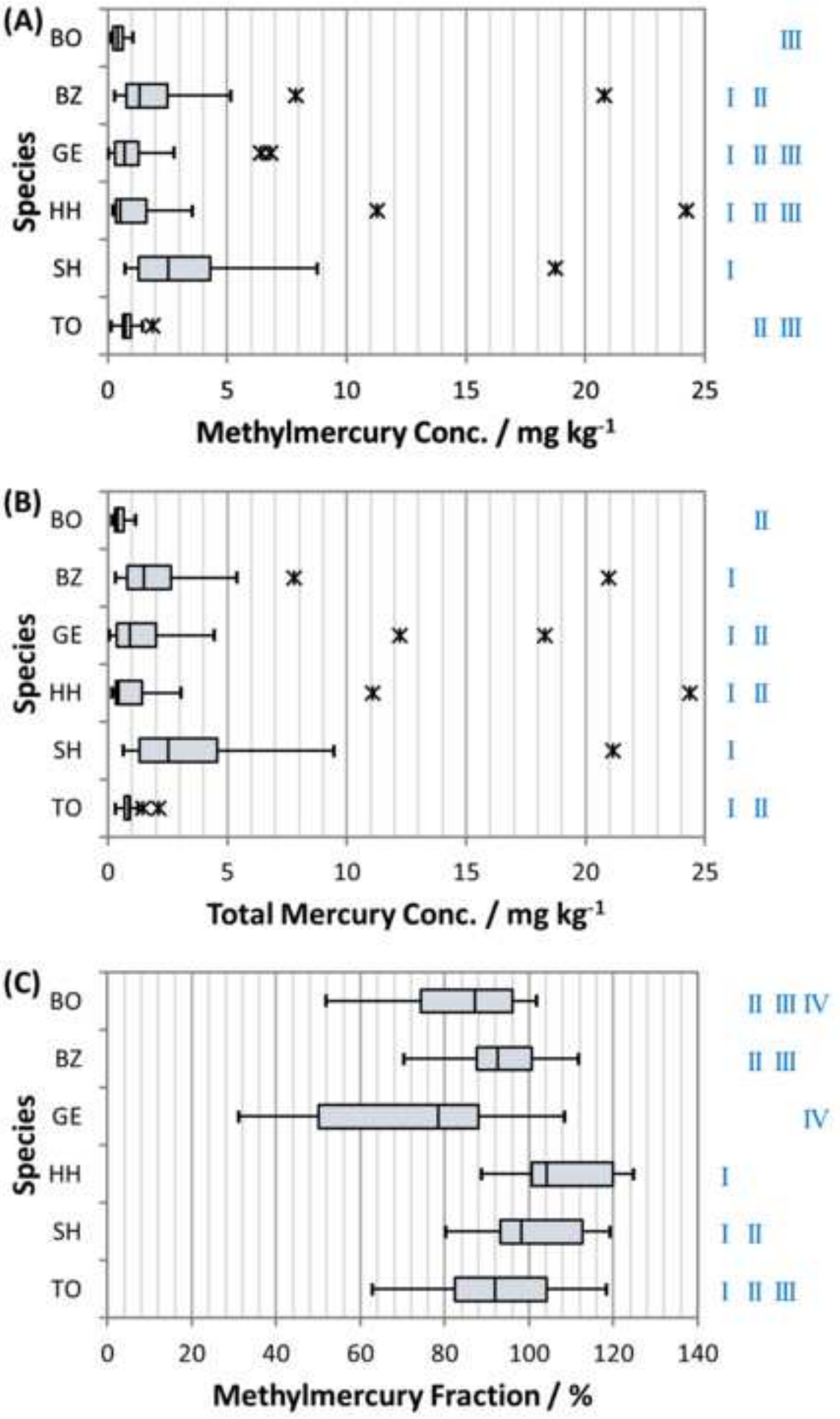

Figure 2

Click here to access/download;Figure;Figure 2.tiff

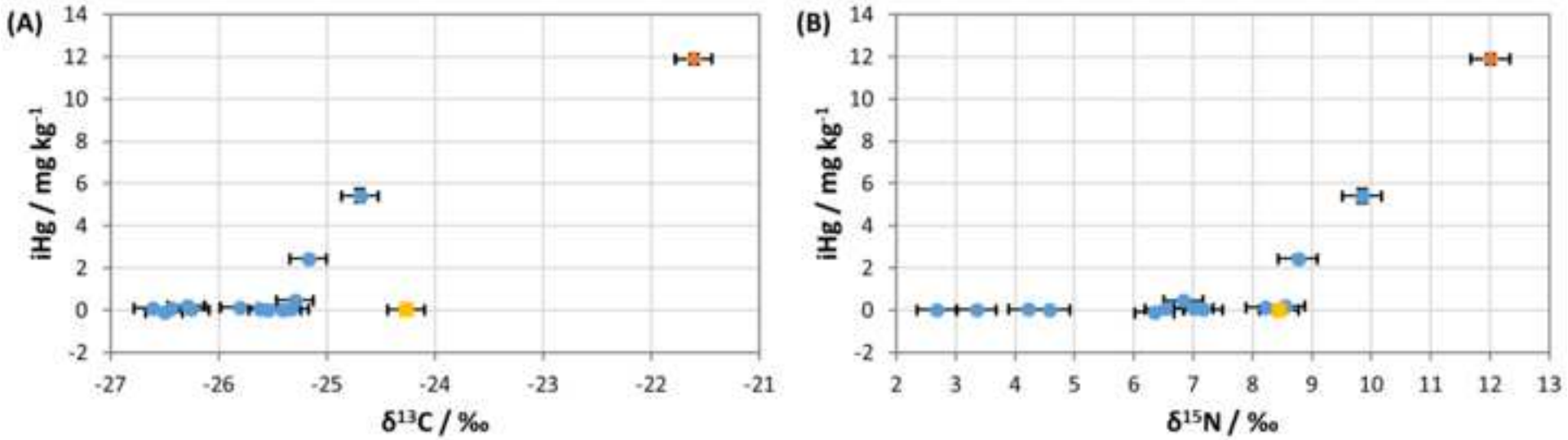

Figure 3

Click here to access/download;Figure;Figure 3.tiff

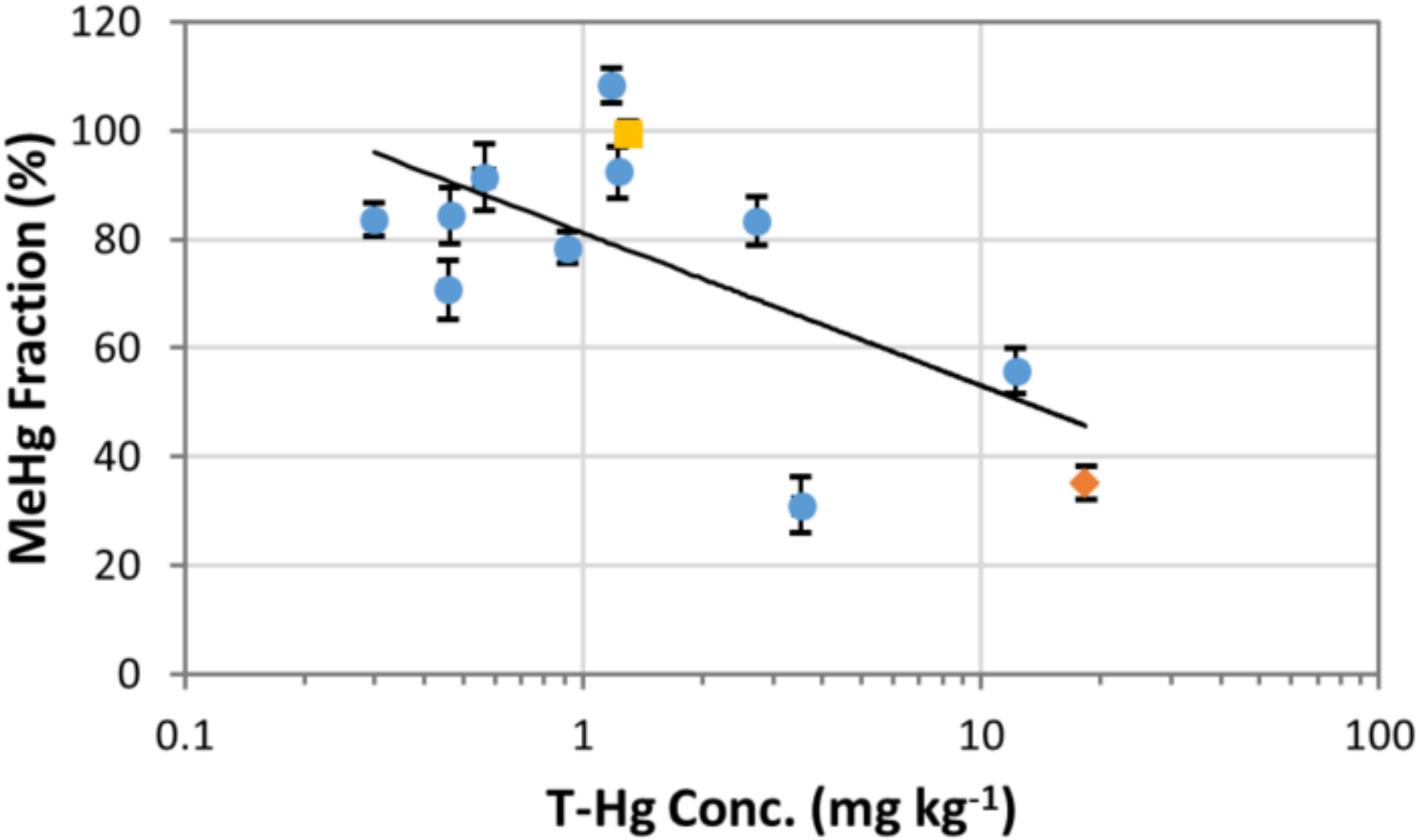

Figure 4

Click here to access/download;Figure;Figure 4.tiff

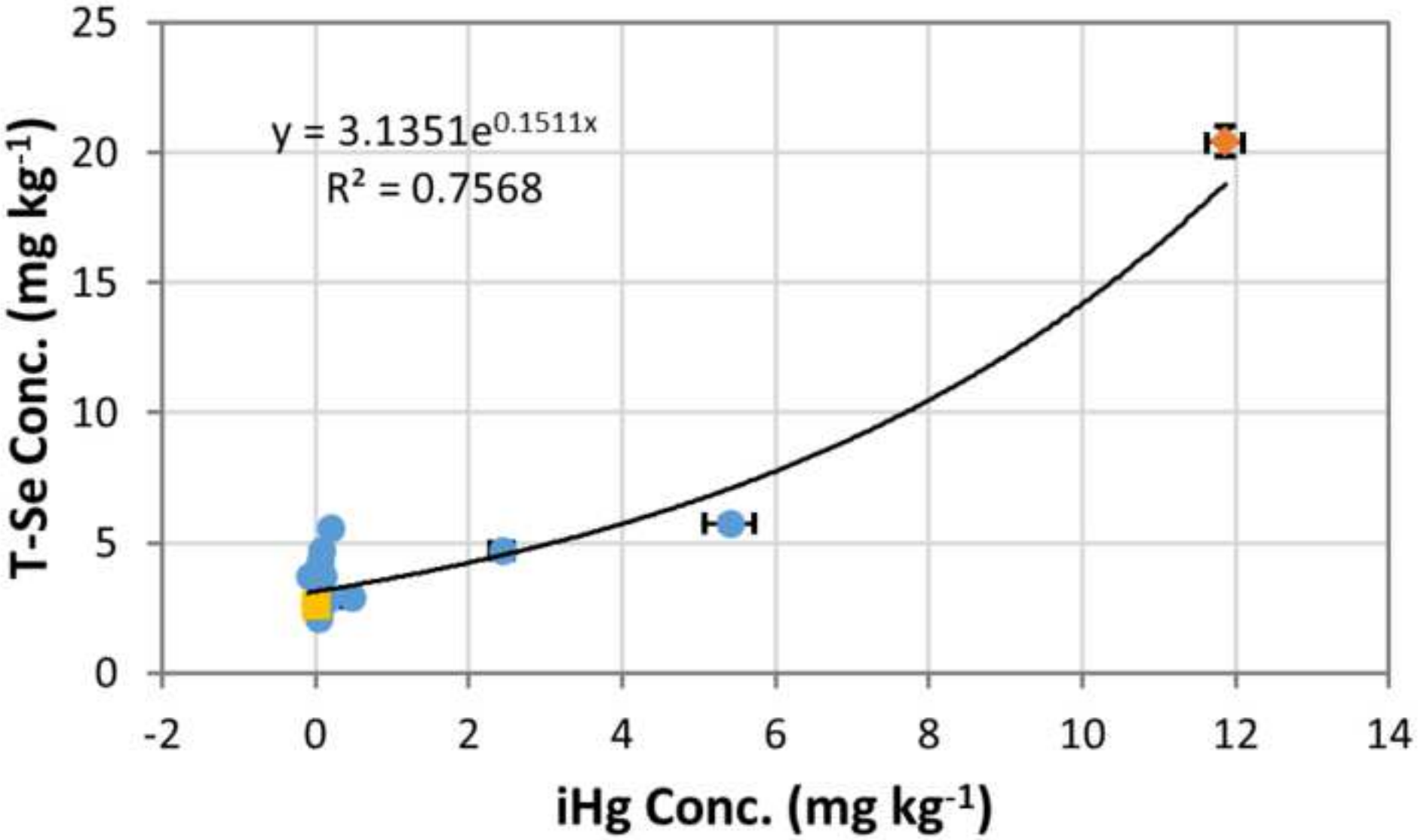

Figure 5

Click here to access/download;Figure;Figure 5.tiff

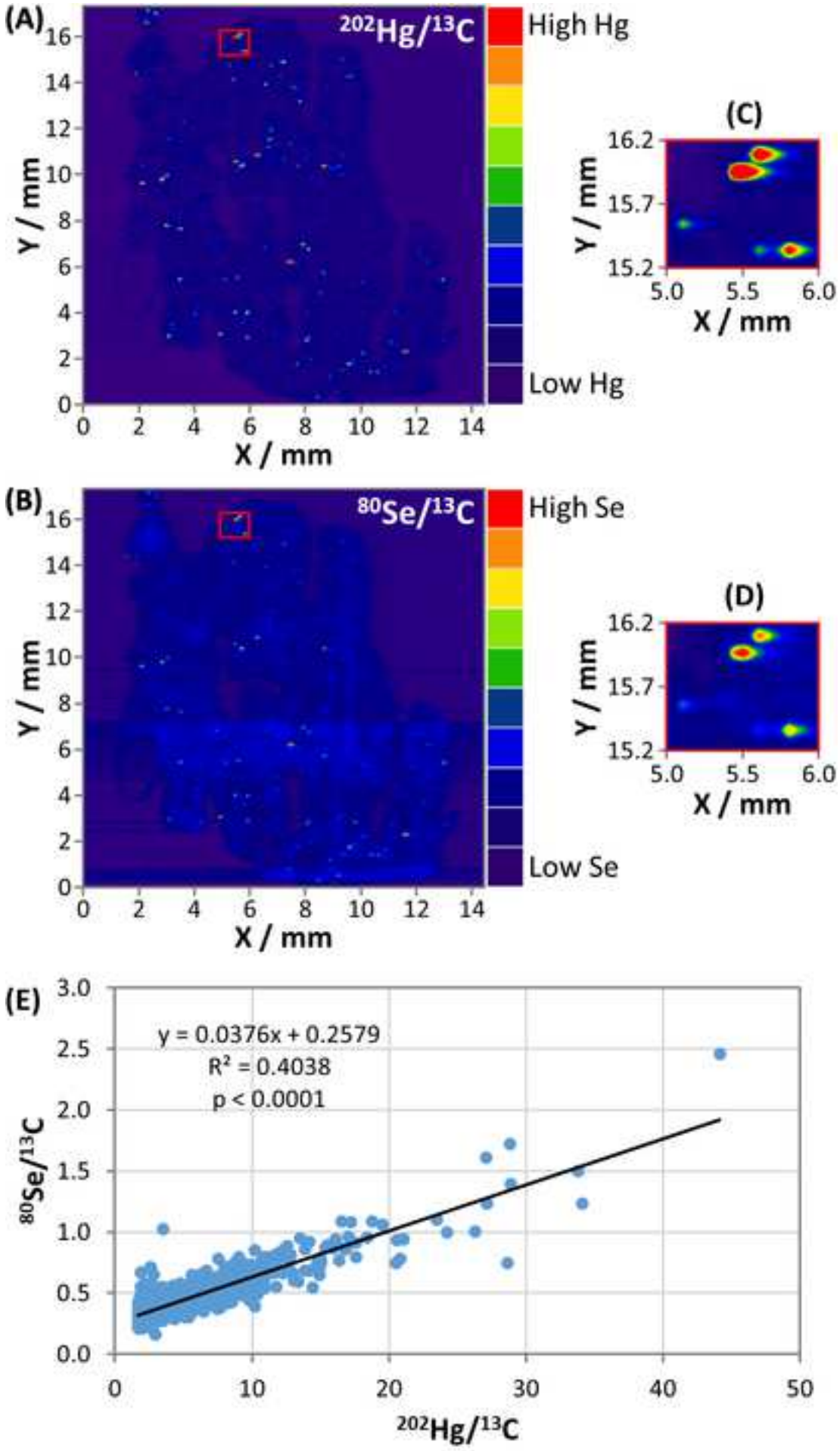

Declaration of interests

☒ The authors declare that they have no known competing financial interests or personal relationships that could have appeared to influence the work reported in this paper.

☐The authors declare the following financial interests/personal relationships which may be considered as potential competing interests:

Author contributions

Shaun T. Lancaster: Performed the measurements of total mercury, methylmercury, total selenium, and sp-ICP-MS. Performed statistical interpretations of results. Lead author of the submitted manuscript. **Gabriela Peniche:** Sample collection and dissection. Provided input on ecological interpretations of results. **Ali Alzahrani:** Performed the nanoparticle analysis by LA-ICP-MS and TEM. **Magdalena Blanz:** Provided input on the interpretation of stable isotope ratios. **Jason Newton:** Performed the analysis of stable isotope ratios. **Mark A. Taggart:** Conceptualisation, supervision, and editing. **Warren T. Corns:** Supervision, and editing. **Eva M. Krupp:** Conceptualisation, supervision, and editing. **Jörg Feldmann:** Conceptualisation, supervision, and editing.